NeuroImage 269 (2023) 119933

Contents lists available at ScienceDirect

NeuroImage

journal homepage: www.elsevier.com/locate/neuroimage

The interacting brain: Dynamic functional connectivity among canonical brain networks dissociates cooperative from competitive social interactions

D.J. Shaw[a,b,*], K. Czekóová[a,c], R. Mareček[d], B. Havlice Špiláková[a], M. Brázdil[a]

[a] Behavioural and Social Neuroscience, Central European Institute of Technology (CEITEC), Masaryk University, Kamenice 5, Brno 625 00, Czech Republic
[b] Department of Psychology, School of Life and Health Sciences, Aston University, Birmingham B4 7ET, UK
[c] Institue of Psychology, Czech Academy of Sciences, Veveří 97, Brno 602 00, Czech Republic
[d] Multimodal and Functional Neuroimaging, Central European Institute of Technology (CEITEC), Masaryk University, Kamenice 5, Brno 625 00, Czech Republic

ARTICLE INFO

Keywords:
Dynamic functional connectivity
Canonical brain networks
Social interaction
Cooperation
Competition

ABSTRACT

We spend much our lives interacting with others in various social contexts. Although we deal with this myriad of interpersonal exchanges with apparent ease, each one relies upon a broad array of sophisticated cognitive processes. Recent research suggests that the cognitive operations supporting interactive behaviour are themselves underpinned by several canonical functional brain networks (CFNs) that integrate dynamically with one another in response to changing situational demands. Dynamic integrations among these CFNs should therefore play a pivotal role in coordinating interpersonal behaviour. Further, different types of interaction should present different demands on cognitive systems, thereby eliciting distinct patterns of dynamism among these CFNs. To investigate this, the present study performed functional magnetic resonance imaging (fMRI) on 30 individuals while they interacted with one another cooperatively or competitively. By applying a novel combination of analytical techniques to these brain imaging data, we identify six states of dynamic functional connectivity characterised by distinct patterns of integration and segregation among specific CFNs that differ systematically between these opposing types of interaction. Moreover, applying these same states to fMRI data acquired from an independent sample engaged in the same kinds of interaction, we were able to classify interpersonal exchanges as cooperative or competitive. These results provide the first direct evidence for the systematic involvement of CFNs during social interactions, which should guide neurocognitive models of interactive behaviour and investigations into biomarkers for the interpersonal dysfunction characterizing many neurological and psychiatric disorders.

1. Introduction

To interact effectively with others and conduct ourselves appropriately in interpersonal contexts, we must perform a broad range of sophisticated cognitive operations in a carefully coordinated manner. Even a fleeting exchange with a stranger, for example, requires us to process multiple social cues simultaneously (e.g., their verbal and non-verbal expressions) to infer their intentions, motivations and emotions, and use this information to adjust our own behaviour in a context-appropriate manner. This is complicated further by the reciprocal nature of social interactions; our fellow interactant(s) continuously modify their behaviour in response to our own, giving rise to an interpersonal context that evolves unpredictably and imposes time-varying demands on social cognitive systems. To support interactive behaviour, then, the brain must be capable of deploying and switching flexibly between the different functional brain networks that transiently link distributed neural systems underpinning these social cognitive processes. Moreover, the manner in which such dynamic functional connectivity unfolds should reflect the specific type of social exchange being supported; distinct forms of interaction will impose different demands on cognitive systems, requiring distinct patterns of reconfiguration among functional brain networks. The present study investigated this by examining if opposing types of social interaction give rise to systematic patterns of dynamic functional brain connectivity.

High-level cognitive operations are underpinned by widespread and often overlapping brain networks that connect discrete neural systems (Braun et al., 2015; Bressler and Menon, 2010; Gonzalez-Castillo and Bandettini, 2018). This is true particularly for social cognitive processes. Meta-analytic data indicate that inferences about others' mental (e.g., intentional) states are supported by a diffuse brain network encompassing medial and ventro-lateral prefrontal as well as temporo-parietal cortices (Molenberghs et al., 2016; Schurz et al., 2013). Similarly, inferring and sharing in others' affective states (empathy) recruits a network comprising medial and ventro-lateral prefrontal cortices, anterior insu-

* Corresponding author at: Department of Psychology, School of Life and Health Sciences, Aston University, Birmingham B4 7ET, UK.
E-mail address: d.j.shaw@aston.ac.uk (D.J. Shaw).

https://doi.org/10.1016/j.neuroimage.2023.119933.
Received 19 October 2022; Received in revised form 20 January 2023; Accepted 4 February 2023
Available online 6 February 2023.

lae and inferior parietal cortices (Arioli et al., 2021; Lamm et al., 2011; Timmers et al., 2018); and processing the actions of others engages a network consisting largely of lateral prefrontal and inferior parietal cortices (Diveica et al., 2021; Hardwick et al., 2018). The overlap among these neural systems engaged during social cognitive processes appears to reflect the common involvement of canonical functional brain networks (CFNs; Feng et al. 2021, Schurz et al. 2020) - stable, intrinsically connected neural circuits linking distributed brain regions. Dynamic integrations among CFNs are believed to subserve more foundational cognitive processes that together orchestrate adaptive behaviour in both social *and* non-social domains (Menon and D'Esposito, 2022; Uddin et al., 2019). One example is the lateral fronto-parietal network (or central executive system) - a set of frontal and parietal structures that are functionally coupled during a diverse range of general-purpose cognitive processes (e.g., working memory, task switching; Assem et al. 2019, Duncan 2010, Seeley et al. 2007). Another is the default mode network - inter-connected brain regions spanning medial and lateral parietal, medial prefrontal, and medial and lateral temporal cortices. Within this network, brain activity is suppressed during externally oriented attention but increased during internal mentation (e.g., autobiographical memory retrieval; Buckner and DiNicola 2019, Raichle 2015, Raichle et al. 2001). Social cognitive processes also engage core nodes of three distinct brain networks that operate in concert to control the allocation of attention: the ventral attention network, consisting of ventro-lateral prefrontal and temporo-parietal cortices; the dorsal attention network, comprising dorso-lateral prefrontal and parietal cortices (Vossel et al., 2014); and the salience network, encompassing anterior insulae, dorsal anterior cingulate and various subcortical structures (Seeley et al., 2007).

Given the extensive overlap between functional brain networks implicated in social and domain-general cognitive processes, it might be that the latter provide fundamental support to higher-level social cognition and interactive behaviour (e.g., Binney and Ramsey 2020a). Recent meta-analyses support this notion: Schurz et al. (2020) report that social cognitive processes, such as inferences concerning others' intentional states, appear to involve a balanced interplay of functional integration and segregation among several CFNs. Likewise, Feng et al. (2021) identify many of the aforementioned CFNs from a synthesis of brain imaging investigations into social interaction, and their functional profiling suggests a role of general-purpose cognitive processes during interactive behaviour (e.g., working memory). Importantly, however, these meta-analytic studies provide only static snapshots of CFN involvement during social cognition and interactive behaviour, providing little insight into their dynamic involvement; it remains to be seen how dynamic connectivity among these functional brain networks unfold during social interactions, or if discrete types of interpersonal exchange elicit dissociable patterns of dynamism among them. The present study investigated if and how systematic patterns of dynamic functional connectivity (integration and segregation) among CFNs are elicited during different types of interpersonal behaviour.

Various analytical techniques have been developed to capture time-varying changes in functional brain connectivity from neuroimaging data (Hutchison et al., 2013; Iraji et al., 2021; Lurie et al., 2020). Many are based on a sliding-window approach, whereby a window of fixed length is advanced across a time-series and patterns of covariance among localised signals is estimated within each time segment. Discrete windows of functional connectivity are then subjected to clustering techniques to identify distinct or repeating patterns of covariance that emerge during the entire time-series. Although this approach has revealed time-varying patterns of functional connectivity associated with distinct cognitive operations (reviewed in Iraji et al. 2021), it fails to account for the non-stationarity of functional brain networks; it cannot capture the continuous evolution of brain states over time in response to moment-by-moment changes in task demands (Hutchison et al., 2013), such as those encountered during interpersonal contexts. An alternative approach is offered by state-space models, which seek to identify the latent brain states that generate observed patterns of continuous time-varying co-activations. Latent states are identified in a data-driven and multivariate manner through matrix factorisation, thereby circumventing the need for arbitrarily sized moving windows or temporal boundaries. Furthermore, state-space models estimate various spatio-temporal characteristics of latent states that provide mechanistic insights into the processes generating observed brain dynamics: their underlying functional circuitry, probability of occurrence (occupancy) and stability over time (lifetime), and the probability with which different states transition among one another.

To investigate the dynamic connectivity of CFNs during social interaction, it is necessary to examine them while they operate online during real interpersonal exchanges (Iraji et al., 2021; Redcay and Schilbach, 2019; Schilbach, 2014; Schilbach et al., 2013; Shamay-Tsoory and Mendelsohn, 2019). To achieve this, in the present study we acquired functional brain imaging data from individuals while they performed the interactive Pattern Game (iPG; Špiláková et al. 2019, 2020) - a joint-action task in which pairs of individuals interact with one another interdependently across a series of exchanges, in either a cooperative or competitive manner. Since both interactants necessarily have a mutually reciprocal influence on each other's behaviour, each round of interpersonal exchanges evolves unpredictably and progressively. In a simple adaptation of this task, we also allowed players to determine the nature of a given interaction by choosing whether to cooperate or compete with one another. The "two-person" set-up of the iPG thereby captures some of the defining characteristics of social interaction (Misaki et al., 2021) that are inaccessible to the "single-person" paradigms utilised commonly in social neuroscience (Hari and Kujala, 2009; Hari et al., 2015); it goes beyond the "spectator science" of measuring the brains of individuals situated in decontextualized environments while they passively observe social stimuli, allowing us instead to investigate the dynamics of brain networks subserving social information processing while they operate in real-time to support social interaction. Achieving such ecological validity is important when we consider neuroscientific research that has shown differences in the way the brain responds during the passive observation of social stimuli compared to when individuals are engaged actively in social interaction (e.g., Alkire et al. 2018, Redcay et al. 2010, for related discussions see Schilbach et al. 2013, Redcay and Schilbach 2019).

By applying a state-based model to brain imaging data acquired from individuals engaged on this adapted iPG, we investigated properties of dynamic functional connectivity among seven well-defined CFNs during interactive behaviour. Since the iPG dissociates cooperative from competitive exchanges, it allowed us to investigate more specifically whether these opposing types of interpersonal context elicited systematic differences in states of dynamism among these brain networks. We then assessed whether states that differentiate systematically among these different types of interaction can be used to predict the type of interaction in which pairs of individuals were engaged in an independent dataset.

2. Methods

2.1. Data availability

All experimental materials, protocol and analysis codes are available publically at https://osf.io/s2jmh/. All fMRI data are available upon request to the corresponding author, following approval for data sharing from the Research Ethics Committee of Masaryk University.

2.2. Participants

Forty individuals (22 males; mean age = 26.45 [SD = 2.84] years) volunteered for the study, all of whom were recruited from Brno, Czechia. Due to a lack of behavioural responses, resulting partly from technical failures, data from 10 of these participants were omitted from

any analyses (see Supplementary Table S1). The remaining 30 individuals (16 males; mean age = 26.03 [SD = 2.41] years) were all right handed, and were paired into 15 same-sex dyads (8 male-male) matched on age (mean intra-dyad difference = 5.07 [SD = 3.78] months) and education (highest qualification achieved). The participants comprising each dyad were unfamiliar with each other prior to the experiment; they were introduced briefly to one another for the first time on day of scanning while they were instructed together about the task and scanning procedure. All participants gave their informed consent prior to the scanning procedure, which was approved by the Research Ethics Committee of Masaryk University. Participation was rewarded with 200 CZK (approx. €8).

2.3. Interactive pattern game

The interactive Pattern Game (iPG; Špiláková et al. 2019b, 2020) is a joint-action task on which two players interact with one another repeatedly over several rounds (trials) to reconstruct various target patterns comprised of blue and yellow tokens. At the beginning of the game, each player was assigned to one of two colours - blue or yellow - which remained fixed throughout. At the start of every round, one player was assigned the role of the Builder whose goal was to recreate a target pattern as closely as possible. Due to the layout of the target patterns, the Builder could never recreate a pattern perfectly on their own; they required supporting tokens to be placed by their co-player - the Other. On interactive rounds, the Other was free to choose either to help the Builder or hinder them from reconstructing the pattern - their only instruction prior to the procedure was to distribute their choices as evenly as possible. This choice defined two types of interactive rounds (conditions): Cooperation (COOP) and Competitive (COMP), respectively. In non-interactive Control (CTRL) rounds, the Other simply observed the Builder attempting to recreate the target pattern, with no opportunity to help or hinder them. Participant roles alternated on each of 32 interactive rounds, such that each player acted as the Builder or Other on an equal number of exchanges. In 16 non-interactive CTRL rounds, the role of lone Builder was played by either the blue or yellow player.

Fig. 1 presents examples of the three round types and a schematic time-course. At the start of each round, an instruction was presented for 3 s that allocated each participant to a player role. On interactive rounds, the Other was then given 4 s to decide whether they would help or hinder the Builder and indicate their decision by way of a button press. The Other's decision was not communicated to the Builder. This was followed immediately by a white fixation cross for 1 s, signaling to the players that a round was about to begin. Every round started with the Builders' first token presented on one side of the stimulus display, above the playing board. The Builder then moved this token either left or right to the desired columnar location before releasing it into the lowest empty row. Tokens were moved *via* a four-button response box operated by both hands. On interactive rounds, the Other's first token was subsequently presented on the opposite side of the stimulus display, and they placed their token in a helpful or hindering position. In every interactive round, each player had five tokens to place within 25 s. Once this time had expired, a new round began regardless of how many tokens remained. The Other received no tokens on CTRL rounds; Builders had 25 s to recreate the target pattern as closely as possible with only their five tokens. Before the scanning session, both participants performed four practice CTRL rounds to familiarise themselves with the task.

The iPG was programmed entirely in MATLAB (v2016b, The MathWorks, Inc.) using the Cogent 2000 toolbox (Cogent 2000 team; Functional Imaging Laboratory and Institute of Cognitive Neuroscience).

2.4. MRI acquisition

Structural and functional brain images were acquired using two identical 3T Siemens Prisma scanners housed within the same facility, each equipped with a 64-channel HeadNeck coil. High resolution T1-weighted anatomical images were first recorded with a MPRAGE sequence (TR/TE = 2000/2.33 msec; flip angle = 8°; matrix = 240 × 224 × 224; 1 mm^3 voxels). Functional time-series were then recorded in a single run containing 600 volumes (~20 min). Blood oxygen-level dependent (BOLD) images were obtained with T2*-weighted echo planar imaging with parallel acquisition (i-PAT; GRAPPA acceleration factor = 2; 34 axial slices; TR/TE = 2000/35 msec; flip angle = 60°; matrix = 68 × 68 × 34; 3 × 3 × 4 mm voxels). Axial slices were acquired in interleaved order, and synchronised between the two scanners by way of an external programmable signal generator (Siglent SDG1025; www.siglent.com). Both scanners were connected to a single stimulation computer.

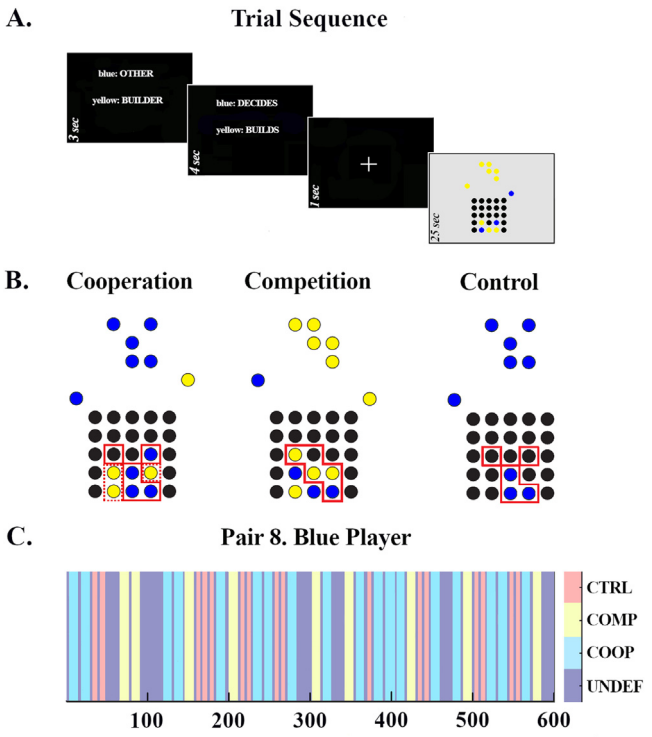

Fig. 1. The interactive Pattern Game. *A*: Schematic of round (trial) structure. *B*: Examples target patterns and required token placements in cooperative (COOP), competitive (COMP), and non-interactive control (CTRL) rounds. In all examples, the Builder is assigned the same colour as the target pattern located above the playing board, and scores by placing tokens in locations that recreate the pattern (indicated by solid red lines). In COOP and COMP rounds, the Other scores by placing their tokens in locations that serve to help (dashed red lines) or hinder the Builder; since the latter is achieved by placing tokens within the pattern space, thereby obstructing the Builder, the scoring location of Others and Builders are the same in COMP rounds. *C*: Example event sequence from one pair, showing the even distribution of round types determined by Others' choices, and undefined rounds (UNDEF) in which Others did not indicate their choice with a button press. *Note*: this event sequence had the highest autocorrelation of all the pairs, showing a fairly even distribution of rounds types even in this worst case.

2.5. Pre-processing

Using FEAT v6.00, functional time-series were high-pass filtered across time (Gaussian-weighted least-squares straight line fitting; sigma 50.0 s), spatially smoothed using an 5 mm FWHM Gaussian kernel, slice-time corrected for interleaved acquisition, and intensity normalized using grand-mean scaling of the entire 4D dataset by a single multiplicative factor to minimize unspecific time effects. Functional time-series were motion corrected using MCFLIRT (Jenkinson et al., 2002). Given the detrimental effect of residual motion artifacts on measures

of functional connectivity (Power et al., 2015; van Dijk et al., 2012), and to minimise the occurrence of spurious dynamics resulting from covarying physiological sources (e.g., heart rate, respiration; Gonzalez-Castillo and Bandettini 2018), we also identified and removed any such artifactual signals: using MELODIC (Beckmann, 2012; Beckmann et al., 2004), we applied a probabilistic independent component analysis (ICA) to decompose the time-series into 50 independent spatial and temporal components. Artifactual components were then identified automatically with the Spatially Organized Component Klassifikator (SOCK; Bhaganagarapu et al. 2013, 2014), and signal relating to these nuisance covariates were regressed from the time-series using the *fsl_regfilt* utility. Importantly, dyad-specific event sequences (onsets and durations of round types) were entered into the ICA applied to each pair of time-series, and post-hoc regression analyses ensured that no task-related component was classified as artifactual. Although other ICA-based strategies for the removal of artifactual signals have been shown to outperform SOCK in terms of sensitivity to detect motion-related signals, it is more effective than nuisance regression and highly reliable in its detection of remaining CFNs (Pruim et al., 2015).

2.6. Regions of interest

From the pre-processed functional images, we extracted average time-series across all voxels contained within each of the 400 non-overlapping elements of the cortical parcellation from Schaefer et al. (2018). Derived from a fusion of local gradient and global similarity approaches, each cortical parcel expresses high connectional homogeneity - that is, all voxels assigned to a given parcel exhibit similar patterns of connectivity with the rest of the brain. Moreover, this parcellation preserves the topographical structure of seven CFNs detected reliably in the brain at rest (Yeo et al., 2011): it encompasses every cortical node of the visual (Vis) and somatomotor network (SM), dorsal and ventral attention networks (DAN and VAN), limbic network (Lim), fronto-parietal network (FP) and the default mode network (DMN). This parcellation therefore allowed us to examine the relative involvement of these seven CFNs, and dynamism among them, during interactive behaviour.

2.7. Dynamic functional connectivity

State-based analyses of dynamic functional connectivity are grounded in the general framework of probabilistic generative models. Belonging to the class of matrix factorisation models, they assume that the observed data extracted from regions of interest at any one time-point are generated from latent source factors (states) with lower dimensionality in a latent subspace, together with measurement noise. Identification of these latent factors is achieved with vector autoregressive and factor analysis models. The optimal number of latent states is determined from the data using Bayesian model selection, which penalises excessively complex models. The observed brain data at each time point are then generated as the summation of activity of several latent states.

To identify latent states and estimate their temporal evolution during interactive behaviour on the iPG, we applied Bayesian Mixture of Factor Analysers (BMFA; Ghahramani and Beai 2000) to the entire time-series (all 600 volumes) extracted from each of the 400 regions of interest across all 30 participants. This analytical technique models the observed data at a given time-point as a weighted average of factor analyser densities. A recent extension to BMFA applies hidden Markov models to infer the structure of the latent subspace (Taghia et al., 2017, 2018); hidden latent states are linked together through a first-order Markov chain, with an implicit assumption that the stochastic rule of state transitions depends only on the last state. This temporal assumption has yet to be confirmed with lower frequency fMRI data acquisition, however, and any deviation from this assumed Markovian temporal structure might be detrimental to such modelling. Since BMFA does not assume any temporal dependencies among states, is it influenced less by sampling frequency. Indeed, it has been shown that the accuracy of estimation achieved by mixture models is comparable to, and sometimes better than, hidden Markov models applied to data acquired with lower sampling frequencies such as that used in the present study, particularly with small sample sizes (Ezaki et al., 2021).

In BMFA, the number of states to be extracted must be set *a priori*. We determined the optimal model structure (number of states) using a general criterion: BMFA was computed with variational Bayesian approximation for 2 to 30 states, each number of states estimated 10 times with random initialisations and estimation convergence controlled by Free Energy and parameter change. The optimal number was then determined by identifying the point at which the change in Free Energy (improvement in model fit) was too small to justify higher model complexity (an increase in the number of states). As a verification of this approach, we also computed several metrics employed commonly to evaluate the optimal solution of cluster analyses: silhouette and point-biserial correlation coefficients, and Davies-Bouldin, Calinski-Harabasz and Dunn indices.

For each of the optimal set of states, BMFA estimated its group-level pattern of covariance among the 400 regions of interest and its posterior probability at each time point. We then segmented its time-course of occurrence probability into the three types of iPG rounds (COOP, COMP and CTRL) before concatenating these segments into player- (Builder and Other) and condition-specific time-series. Rounds in which Others failed to communicate if they were cooperating or competing (Undefined) were omitted from this process and all subsequent analyses. From these concatenated time-courses, we calculated the average evolution of a given state together with its occupancy, lifetime, and transition probability (see Supplementary Fig. S1). For each volume of the concatenated time-courses, the dominant state was determined as the one with the highest probability of occurrence (winner-takes-all approach). The concatenated time-series were then divided into epochs in which a dominant state was sustained, from which the three temporal characteristics were computed. Occupancy during each condition was calculated as the proportion of epochs in a concatenated time-series expressing a given state to the number of all epochs, and lifetime was calculated as the mean duration of epochs expressing that state. The transition probability among states was calculated across the entire concatenated time-series, on a volume-by-volume rather than epoch basis. Importantly, the between-state transitions were computed only from scans acquired consecutively under the same condition - not across concatenated scans.

2.8. Partial least-squares

Next, we assessed whether the three temporal characteristics for each state differed systematically between player roles and/or round types. For each of the 30 participants, we computed role- and condition-specific S-dimensional vectors for occupancy and lifetime, where S is the optimal number of states, and SxS matrices of state transition probabilities. To identify differences or commonalities in the expression of states during each type of player role and round type, we subjected these three sets of vectors and matrices to Partial Least-Squares (PLS) analysis (e.g., McIntosh et al. 1996, McIntosh and Lobaugh 2004). For each of the three temporal characteristics, six condition- and role-specific matrices were created comprising 30 (participant) rows and columns containing vectorised occurrence probabilities or lifetimes for each state, or between-state transition probabilities. These six matrices were then stacked together to form a single data matrix, which was adjusted to remove subject-specific effects; specifically, the mean across all six matrices belonging to a particular subject were subtracted from each constituent matrix. The PLS analysis computed a new cross-block matrix, M, that defined the covariance among the six condition- and role-specific matrices for each metric. Through singular value decomposition of M, a set of latent variables (LV) emerged that each identified a particular pattern of covariance among the input matrices: one element of

each LV contains numerical weights (saliences) for each input matrix, creating a profile that represents the pattern of covariance (i.e. commonalities or differences) across conditions and roles. The other element of the LV — the 'singular image' — identifies the cells of M (i.e. data values) that together covary across the conditions in a pattern aligned with the saliences. In other words, for each temporal characteristic, each LV identifies a pattern of covariance among the states that changes in a coordinated fashion across conditions and player roles.

To assess the statistical significance of the emerging LVs, permutations were used to rearrange the input matrices; specifically, 10,000 permutations reorganised the participant rows while holding constant the data columns. This results in a distribution of new singular values, which are used as a null hypothesis against which the original singular values are compared (Krishnan et al., 2011; McIntosh and Lobaugh, 2004). To test the reliability of the data elements, bootstrapping was used to create entirely new sets of data by sampling with replacement. By dividing the mean of the distribution by its standard error, bootstrap ratios were derived; the larger the ratio, the more stable the data value. Bootstrap ratios can then be expressed as z-scores, and considered significant at $z>1.96$ (equivalent to $p<.05$).

2.9. Cross-validation

We evaluated the robustness of LVs emerging from the PLS analyses by performing a cross-validation on an independent dataset. Specifically, we assessed whether the temporal characteristics of states that differentiated reliably between rounds types in the present study could be used as a training dataset to classify the type of interaction taking place in a test dataset acquired from an independent sample. The test dataset is described fully in Špiláková et al. (2020). In brief, 38 individuals (22 males; mean age = 22.44 [SD = 1.90] years) underwent two runs of fMRI whilst they interacted in pairs on a slightly different version of the iPG. One of these runs was used as the test dataset for this cross-validation - the run in which pairs interacted in a turn-based fashion on a version of the iPG that was identical in every way to the current adaptation except that Others were instructed to help or hinder on each round rather than choosing themselves. Functional brain images were acquired with the same 3T Siemens Prisma scanners using identical image acquisition parameters.

We created the test dataset in same way as the training dataset: for each of the optimal set of states emerging from the BMFA analysis of the 30 functional brain images acquired in the present study, we estimated its posterior probability at each time point of the 38 functional brain images acquired in the previous study. As before, we then segmented each of the resulting 38 probability time-courses into the three types of iPG rounds (COOP, COMP and CTRL) before concatenating these segments into role- (Builder and Other) and condition-specific time-courses. For each of the 38 subjects and both player roles, we then averaged the probability time-course for each state across all rounds of a particular condition. The test dataset then comprised 228 samples for each state (19 pairs x 2 players x 2 roles x 3 conditions). In the exact same manner, the training dataset comprised 180 samples for each state (15 pairs x 2 players x 2 roles x 3 conditions).

The training procedure was performed in the Classification Learner Application of MATLAB, using a 5-fold validation scheme and all the constituent classification models: decision trees, discriminant analysis, support vector machines, logistic regression, nearest neighbours, naive Bayes, kernel approximation, ensembles, and neural networks. Features for training the classification models were selected from elements of singular images associated with each of the three PLS analyses that differentiated maximally among COOP, COMP and CTRL rounds in the training dataset. The classificator with the highest estimated classification accuracy was used to predict the type of round from which the test dataset had been acquired.

Table 1
Average frequency and durations of interaction types.

	COOP	COMP	CTRL
Frequency	17.7 (±1.6)	13.5 (±1.7)	16.0 (±0.0)
Round Duration (sec)	19.6 (±2.0)	21.3 (±1.1)	10.0 (±1.8)
Total Duration (sec)	347 (±37)	286 (±37)	160 (±13)

3. Results

Across all 30 participants, the mean (± standard deviation) frequency with which each type of interaction was encountered and the amount of time spent within them is provided in Table 1. To assess the distribution of Others' choices throughout the course of the iPG, we computed the one-lag correlation of binarised event sequences from each pair (1=COOP, 0=COMP; CTRL rounds were pseudo-randomly interspersed throughout the event sequence). The median autocorrelation was 0.13, and the highest (worst case) was 0.37. This demonstrates that Others' choices to cooperate or compete were distributed evenly across the scanning procedure, even in the worst case (see Fig. 1).

3.1. Latent states of dynamic functional connectivity

Inspection of the relative change in Free Energy with increasing model complexity indicated that six latent states were optimal. This converged with the first peaks of the silhouette and point-biseral correlation coefficients, and the Calinski-Harabasz index (see Supplementary Fig. S2). The matrices of Fig. 2A present distinct patterns of covariance among all 400 ROIs captured by each of these six states. Fig. 2B illustrates the mean (and standard deviation) temporal evolution of each states' probability of occurrence over the course of each interaction type for each player role, across all participants. Since all rounds had variable durations determined by players' performance, we resampled the epochs to a common time interval from 0 to 1 (beginning and end of the round) before averaging. To assess the impact of hemodynamic delay on the calculation of states' temporal characteristics and any subsequent analyses, we performed a direct comparison of occupancy, lifetime and transition probability across participants when computed from concatenated condition- and player-specific time-series with and without the inclusion of the first two volumes (4 secs post onset). All characteristics were highly similar when calculated from either dataset (see Supplementary Fig. F3), indicating that any hemodynamic delay had little to no influence. Fig. 3 presents the results of PLS analyses applied to the matrices for each temporal characteristic, from which emerged two significant LVs for occupancy ($LV1_{Occ}$, $p<.001$; $LV2_{Occ}$, $p<.001$), two for lifetime ($LV1_{Life}$, $p<.001$; $LV2_{Life}$, $p=.020$), and two for between-state transitions ($LV1_{Trans}$, $p<.001$; $LV2_{Trans}$, $p=.001$). Below we describe the results for each state separately.

State 1 is characterized primarily by positive covariance among bilateral DMN and Vis network, but also the left FP network. $LV1_{Occ}$ reveals that this state occurs with much higher probability in Builders relative to Others during CTRL rounds, and marginally so in COMP rounds, but the reverse is true during COOP rounds. A similar pattern is revealed by $LV1_{Trans}$; all transitions from and to State 1 occur with much higher probability in Builders relative to Others during CTRL rounds and, to a lesser extent, COMP rounds. A different pattern is revealed by $LV2_{Trans}$, however; in both player roles, transitions to State 1 from State 4 are more probable during CTRL rounds relative to COOP and COMP rounds. This aligns with the shortest stability (lifetime) of State 4 during CTRL rounds (see below). The PLS analysis indicated that the lifetime characteristic of State 1 does not differentiate reliably between player roles or round types.

State 2 captures a pattern of positive covariance among bilateral VAN, DAN, left FP network and, to lesser extent, right FP network and left DMN. The occupancy and between-state transitions involving this

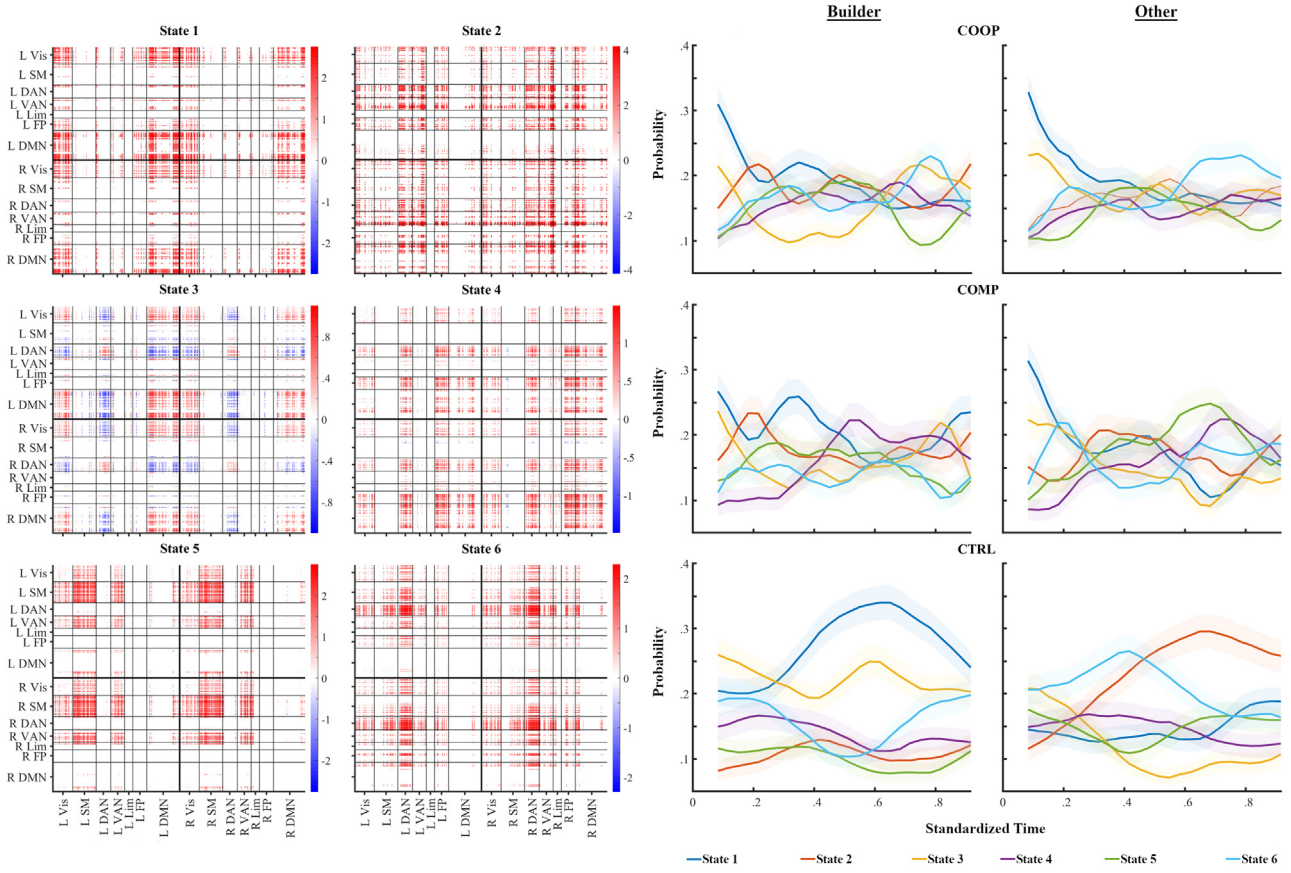

Fig. 2. States emerging from BMFA. *A*: Covariances among all 400 ROIs captured by each of the six states, organised by the canonical functional brain network to which they belong in each hemisphere. *B*: Each states' mean (±SD) posterior probability across the whole sample (*N*=30), plotted across a standardised round of each condition type and separately for each player role.

state show a directly opposing pattern to State 1: $LV1_{Occ}$ reveals that State 2 has a far greater probability of occurrence in Others compared with Builders during CTRL rounds, and a marginally so during COMP rounds, but the reverse is true in COOP rounds. $LV1_{Trans}$ shows a similar pattern of differentiation between player roles in all but one of the transitions from and to State 2, the exception being those between State 2 and 3 that happen with higher probability in Builders relative to Others during CTRL and COMP rounds. Interestingly, the lifetime of State 2 and some of its between-state transitions also differentiate between round types: $LV1_{Life}$ shows that this state occurs with greater stability for both player roles during COMP rounds compared with both COOP and CTRL rounds, and $LV2_{Trans}$ shows that transitions to State 2 from State 6 are least probable during COMP rounds.

State 3 identifies a pattern of positive covariance among bilateral DMN and Vis networks, similar to State 1, but also their negative covariance with the DAN and (to a lesser extent) the left SM network. The occupancy of this state differentiates between player roles in a way mirroring that of State 1, and $LV2_{Life}$ reveals that its lifetime is shortest in Others during CTRL rounds. $LV1_{Trans}$ reveals transitions from and to State 3 that also differentiate player roles in a way that mirrors those involving State 1, but $LV2_{Trans}$ shows a pattern of differentiations among round types; for both players, transitions from State 3 to State 5 are more probable during COMP and COOP (interactive) rounds compared with CTRL rounds, while those to State 6 show the reverse pattern.

State 4 captures a pattern of positive covariance among the bilateral DMN, DAN, Vis and FP networks, and their negative covariance with the right (but not left) SM network. The occupancy of this state does not differentiate reliably between player roles or round types. However, the lifetime of State 4 differentiates among round types in the same way as State 2 - it occurs with greater stability for both player roles during COMP rounds compared with both COOP and CTRL rounds. Transitions involving State 4 reveal a similar pattern of differentiation among round types, but also between player roles: $LV1_{Trans}$ shows that transitions from State 4 to State 1 differentiate between player roles in a fashion similar to the occupancy characteristic of State 1, while its transitions to State 2 and 5 differentiate between player roles in a similar way as the occupancy of those states (see below). $LV2_{Trans}$ shows that transitions from State 4 to State 1 also differentiate between round types, but in an opposite way to the lifetime characteristic of State 4. In other words, the greater stability of State 4 during COMP rounds means that it transitions less with other states during these interactions.

State 5 is represented by a pattern of positive covariance among bilateral VAN, SM and Vis networks. In a pattern that mirrors State 2, the occupancy of State 5 differentiates between player roles while its lifetime characteristic differentiates among round types. Similarly, $LV1_{Trans}$ reveals that all transitions to and from State 5 show a pattern of differentiation among player roles that mirrors those involving State 2. Unlike State 2, however, $LV2_{Trans}$ reveals that transitions to State 5 from State 3 differentiate among round types - they are more probable during COMP compared with COOP and CTRL rounds.

Finally, State 6 captures a pattern of positive covariance among the bilateral DAN, SM and Vis networks, and, to a lesser extent, the VAN and FP network. State 6 shows a unique pattern of differentiation among round types - for both players, it has the highest probability of occurrence during CTRL rounds, but the highest stability during COMP rounds. As mentioned above, $LV1_{Trans}$ captures transitions among State 6 and State 1 that differentiate between player roles in manner consistent with the latter's occupancy profile. The same is true for transitions

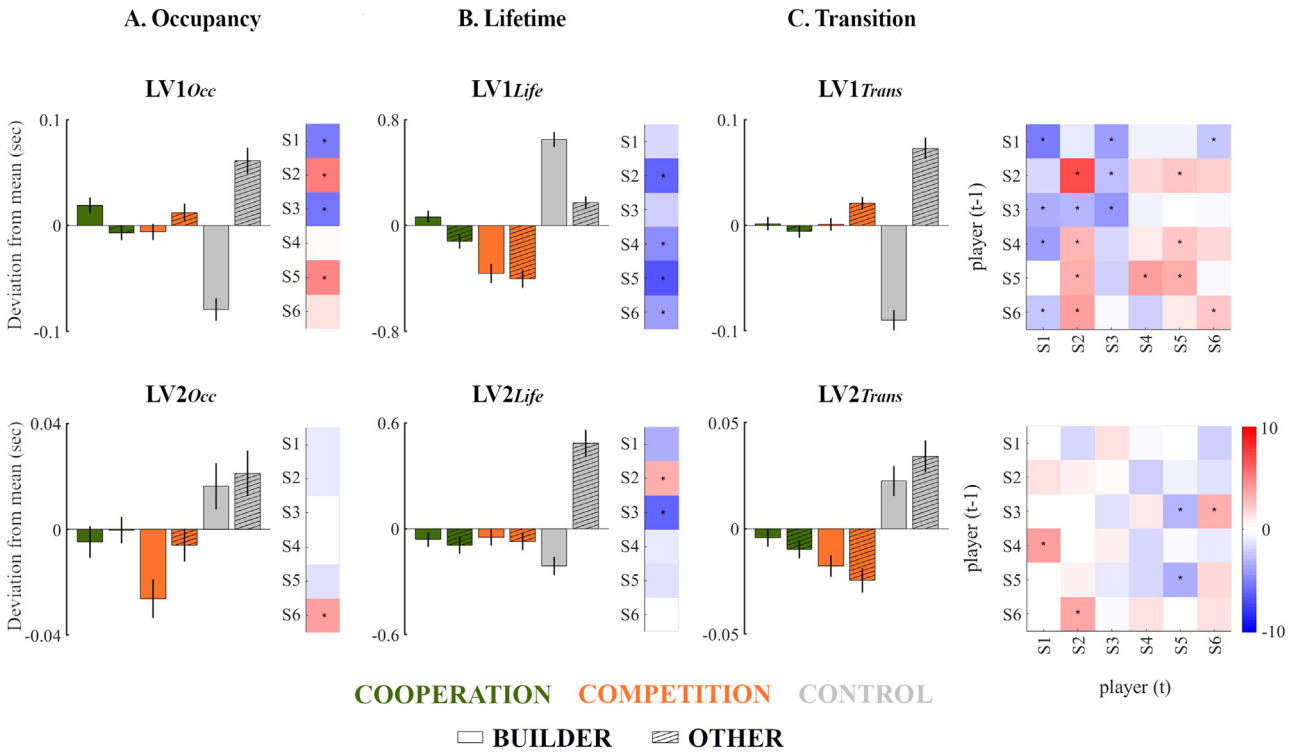

Fig. 3. Systematic patterns of dynamic functional connectivity. This image illustrates results from the separate partial least-squares analyses applied to the occupancy (*A*), lifetime (*B*) and between-state transition probability matrices (*C*). Two significant latent variables (LVs; *p*-values <0.02) emerged from each analysis. For each LV, the bar graph plots saliences across the three conditions (COOP, COMP and CTRL) for each player (Builder and Other), expressed as a deviation from the overall mean; the adjacent vector presents bootstrapped singular values that identify states expressing this pattern significantly (z>1.96, p<0.05). States with positive bootstrap values are correlated positively with the profile of saliences, and those with negative values are correlated negatively with that profile. Together, these pairs of plots illustrates the six states' occupancy, lifetime or between-state transition probability across conditions for each player role.

Table 2
Performance of the support vector machine classification.

		Predicted		
		COOP	COMP	CTRL
True	COOP	**44**	**22**	**10**
	COMP	**32**	**39**	**5**
	CTRL	**10**	**9**	**57**

from State 6 to State 2. However, $LV2_{Trans}$ reveals transitions involving State 6 that differentiate among round types; those from State 3 and to State 2 are most probable during CTRL relative to COMP and COOP rounds, possibly reflecting the longer lifetimes of these states during interactive rounds.

In summary, all states expressed one or more temporal properties that differed systematically among types of round: the occupancy of State 6 ($LV2_{Occ}$), the lifetime of State 2, 4, 5 and 6 ($LV2_{Occ}$), and certain between-state transitions among State 3, 4, 5 and 6.

3.2. Cross-validation

To validate the results of the BMFA and PLS analyses, the ten significant cells from the singular images of the aforementioned LVs were selected as features for training classification models (see Supplementary Fig. S4). The Support Vector Machine (Medium Gaussian) achieved the highest estimation accuracy during the training process (60.6%), and when applied subsequently to the test dataset it correctly classified 61.4% of rounds as COOP, COMP or CTRL (specificity=0.80, sensitivity=0.61; see Table 2). This classification accuracy was significantly higher than chance (No Information Rate = 33.3%; p<.001; exact binomial test).

4. Discussion

The present study investigated the nature of dynamic functional brain connectivity during distinct types of interactive behaviour. Specifically, we examined if and how systematic patterns of dynamism among seven well-established canonical functional brain networks (CFNs) are elicited during cooperative and competitive interactions. To do so, we applied state-based analyses of functional connectivity to brain imaging data acquired from individuals engaged in an interactive task that captures many of the defining properties of naturalistic social interaction. This revealed two primary findings that together reveal properties of brain chronnectomics during real-world social interaction: First, we identify six latent states of functional connectivity that each capture discrete patterns of integration and segregation among specific CFNs during interactive behaviour. Second, we reveal how the brain switches dynamically among these states in a systematic fashion that dissociates cooperative from competitive interactions. With these temporal characteristics, we predicted with above-chance accuracy the type of interaction taking place between pairs of individuals from an independent dataset. These findings support the emerging view that interactive behaviour is supported by domain-general rather than uniquely social cognitive systems (Binney and Ramsey, 2020b; Ramsey and Ward, 2020), and the static brain networks associated frequently with social cognitive processes represent superordinate approximations of dynamic connectivity among CFNs (Alcalá-López et al., 2018; Barrett and Satpute, 2013; Ciric et al., 2017)

It has long been known that complex cognition involves multiple interacting brain networks (e.g., Bressler and Menon 2010, Mesulam 1990), and so it is unsurprising that this is true for the multitude of high-level cognitive processes supporting interpersonal behaviour (Molapour et al., 2021). Indeed, earlier investi-

gations have shown that the functional brain networks supporting mental state inferences and the processing of others' actions co-activate during social interaction, likely reflecting their mutual dependency (e.g., Ciaramidaro et al. 2014, Redcay and Schilbach 2019, Sperduti et al. 2014). It is also well established that intrinsically connected functional brain networks provide a backbone that constrains the flow of information throughout the brain during cognitive processes (e.g., Cole et al. 2014, 2016). As such, it is also unsurprising to see the involvement of multiple CFNs during social interaction. As reviewed earlier, recent meta-analytic data suggests that cognitive processes deployed during social interaction are supported by distinct patterns of connectivity among the visual (Vis), somatomotor (SM), ventral (VAN) and dorsal attention (DAN), limbic (Lim), fronto-parietal (FP) and default mode (DMN) networks (Feng et al., 2021; Schurz et al., 2020). However, the present study provides the first demonstration of functional connectivity among specific CFNs *during* social interactions, going beyond the snapshots revealed by meta-analytic data. Moreover, the accuracy with which we predicted the type of interactions taking place in an independent dataset using only the temporal characteristics of dynamism among these discrete networks provides strong evidence for their systematic involvement during interpersonal behavior.

The systematic patterns of involvement and transitions among CFNs that we have observed during interpersonal exchanges extend previous findings of their functional connectivity during discrete, general-purpose cognitive processes (for a review, see Gonzalez-Castillo and Bandettini 2018). Three of the states emerging from our analyses capture patterns of functional connectivity that involve the DMN: both State 1 and 3 are characterized primarily by its positive covariance with the Vis network, and the latter also captures its negative covariance with the DAN and left SM network. These two states occur and transition among one another with greatest probability in Builders during control rounds, while they are acting independently. Given the apparent role of dynamic functional connectivity among these networks during sustained attention (Cai et al., 2021; Lee et al., 2022), we interpret these patterns of positive covariance to reflect externally directed attention uninterrupted by the actions of a fellow interactant. The negative covariance ("anti-correlation") among the DAN and the DMN captured by State 3, which was expressed with greatest stability and transitioned to State 1 more frequently in Others while they passively observed the actions of the Builder, has been observed in tasks that require individuals to infer the mental (i.e. belief) states of another agent (e.g., Schuwerk et al. 2014). This pattern of covariance, might therefore reflect shifts from passive observation to active inferences about a player's motivations and intentions to understand and predict their actions.

In contrast, State 4 captured positive covariance among bilateral DMN, DAN, Vis and FP networks, and is expressed with greatest stability during competitive interactions in both players. Functional connectivity between the DMN, DAN and Vis network has been shown to increase during tasks requiring visual attention (Spadone et al., 2015), and tighter integration between the DAN, Vis and FP networks is reported during working memory processes (Kwon et al., 2017). The DAN is also tightly interconnected with the FP network (e.g., Spreng et al. 2010), and positive covariance between these two networks comprise State 2, 4 and 6 - states expressed with greater stability during competitive compared with cooperative interactions. The FP network is also referred to as the "central executive network" (Seeley et al., 2007) given its broad role in executive functions (e.g., working memory, response inhibition, task switching), and is believed to coordinate goal-directed information flow throughout the brain (Uddin et al., 2019). Sitting interposed between the DMN and DAN, and exhibiting fractionation into two subsystems coupled differentially to these adjacent networks, it is suggested that the FP couples flexibly with the DMN or DAN to support rapid task-dependent adjustments in introspective and externally focused visuospatial processes (Dixon et al., 2018). We interpret the greater stability of these states during competitive compared with cooperative exchanges to reflect the greater need for flexible cognition and adaptive behaviour in the former type of interaction, during which both players must react to their co-player's moves.

It is noteworthy that State 2 and 6 involve both the DAN and VAN, with contributions from the DMN and FP network - both are expressed with greatest stability during cooperative rounds. Despite their specialisation for distinct attentional subprocesses, with the DAN performing top-down controlled attentional selection and the VAN involved in the detection of unexpected but behaviorally relevant stimuli, the flexible control of attention required during interpersonal exchanges will presumably necessitate both systems to operate in concert with one another dynamically. Indeed, these systems are observed to be both correlated or anticorrelated depending on task demands (Vossel et al., 2014). It is possible, then, that excitatory projections from the DMN to both the DAN and VAN (Zhou et al., 2018) serve to mediate the recruitment of these two attentional systems to enable adaptive and reciprocal behaviour during interactive exchanges, coordinated by the FP 'control' network to align with task demands.

The involvement of the DMN in four of the six states emerging from our interactive task is perhaps to be expected given its purported role in mediating information transmission between other intrinsic networks and meta-analytic evidence of its involvement during social reasoning (see Schilbach et al. 2008). Core nodes of this network, particularly the temporoparietal junction, precuneus and dorso-medial PFC, are engaged consistently during tasks that require us to represent others' mental states (e.g., their goals and intentions; (Arioli et al., 2021; Li et al., 2014; Van Overwalle, 2009). This is proposed to reflect the role of the DMN in self-projection; by integrating incoming extrinsic inputs with prior intrinsic information through episodic and autobiographical memory retrieval, this network is believed to form context-dependent models of dynamic social situations between the self and others (Yeshurun et al., 2021).

Altered connectivity within the DMN, and its connectivity with other intrinsic networks, might therefore present a biomarker for the disruptions to social cognition and interpersonal dysfunction that characterises many neurological and most - if not all - psychiatric disorders (Cotter et al., 2018; Kennedy and Adolphs, 2012; Schilbach, 2016). Reduced modulation of the DMN and functional connectivity among its hub nodes during social information processing has been reported in schizophrenia and autism spectrum disorder (Du et al., 2016; Hyatt et al., 2020). Further, a meta-analysis of psychiatric disorders by Sha et al. (2019) revealed hypo-connectivity between the DMN and VAN, and between the VAN and FP network, but hyper-connectivity between the DMN and FP and between the DMN and DAN. In this light, the pattern of interconnections we have demonstrated between intrinsically connected canonical brain networks, which differentiate between cooperative and competitive interpersonal behaviours, may go some way towards the definition of a pathoconnectome underpinning the social impairments exhibited by various psychopathologies.

To investigate the involvement of CFNs during interactive behaviour, we employed one of the multi-resolution parcellations provided by (Schaefer et al., 2018) - one generated from (and cross-validated on) the resting-state fMRI data of nearly 1500 brains, and resulting in networks comprising non-overlapping nodes with high functional homogeneity and harmonized to the network structure of (Yeo et al., 2011). This is not the only option available for this purpose, however; flexible parcellations exist that adapt group-level parcels to individual brains (e.g., Mejia et al. 2020), and leverage faster acquisition techniques that improve the reliability of individual-specific parcellations (e.g., Lynch et al. 2020; for reviews see Arslan et al. 2018, Krendl and Betzel 2022, Uddin et al. 2019). Moreover, the 400-node parcellation that we used in the present study might not achieve the same level of functional homogeneity as one of the finer parcellations, and the 7-network topology we selected can be fractionated further into finer sub-systems that express similar levels of stability (Yeo et al., 2011; Urchs et al., 2019). As such, future studies should assess how the findings of the present study compare to those that employ alternative parcellations and fine

network structures. Further research is also needed to determine the directed influence that CFNs exert on one another during social interactions. Only then can we begin to understand their specific contributions to social cognitive processes (Schurz et al., 2020; Zhou et al., 2018). Finally, future studies should build on our increasing understanding of hub nodes in the brain (Menon and D'Esposito, 2022; Molnar-szakacs and Uddin, 2022) to identify those through which CFNs communicate during social interaction.

An important limitation of our study, and one that should be addressed in future research to build upon and extend our findings, is the lack of consideration for behaviours on our interactive task that might be driven by, or give rise to, the dynamic connectivity we have observed among CFNs. In our study, we measured only the number of successful token placements made by each player and the total number of successful recreations of target patterns. Given the relatively low numbers of each metric, we consider them too crude to evaluate against the rich information provided by state-based analyses of dynamic functional connectivity. Future studies should attempt to capture and model the continuous temporal dynamics of players' behaviour on interactive tasks such as the one we have employed. For example, by utilising the version of our interactive task in which players move concurrently rather than in a turn-based manner (Špiláková et al. 2019, 2020), the interdependency of players' moves could be quantified - that is, the degree to which each action is a reaction (consequence) or antecedent to a co-player's behaviour, and how these dependencies might change as leader-follower dynamics emerge. Cross-recurrence quantification analysis (e.g., Wallot and Leonardi 2018) might offer new insights in this regard, making it possible to identify repeating expressions of interactive behaviour during each exchange. Only with richer metrics of interactive behaviour such as these can we begin to understand how inter-network dynamics contribute to interpersonal behaviours.

5. Conclusions

This study has revealed latent states of dynamic functional connectivity comprising patterns of integration and segregation among distinct canonical functional brain networks, the systematic expression and transitions among which distinguished between cooperative and competitive social interactions in two independent datasets. Since these functional brain networks are believed to subserve domain-general cognitive processes, we interpret these findings as evidence that social cognitive processes reflect instantiations of these general-purposes processes, and the static brain networks associated frequently with social cognitive processes represent superordinate approximations of underlying dynamic states. Our findings should direct future research into the pathoconnectome; we have demonstrated the utility of our interactive paradigm and combination of analytical techniques for elucidating biomarkers (i.e. disrupted dynamic functional brain connectivity) of the interpersonal dysfunction characterising many neurological and psychiatric disorders.

Funding

This study has received funding from the Czech Science Foundation (grant number: GA18-21791S). We acknowledge the core facility MAFIL of CEITEC supported by the Czech-BioImaging large RI project (LM2018129 funded by MEYS CR) for their support with obtaining scientific data presented in this paper.

Credit authorship contribution statement

D.J. Shaw: Conceptualization, Methodology, Software, Validation, Formal analysis, Resources, Writing – original draft, Writing – review & editing, Visualization, Supervision, Project administration, Funding acquisition. **K. Czekóová:** Methodology, Software, Resources, Writing – original draft, Writing – review & editing, Project administration, Funding acquisition. **R. Mareček:** Formal analysis, Writing – review & editing, Visualization. **B. Havlice Špiláková:** Conceptualization, Methodology, Software, Investigation, Data curation. **M. Brázdil:** Resources, Writing – review & editing, Supervision, Project administration.

Data availability

Data will be made available on request.

All experimental materials, protocol and analysis codes are available publically at https://osf.io/s2jmh/. All fMRI data are available upon request to the corresponding author, following approval for data sharing from the Research Ethics Committee of Masaryk University.

Supplementary materials

Supplementary material associated with this article can be found, in the online version, at doi:10.1016/j.neuroimage.2023.119933.

References

Alcalá-López, D., Smallwood, J., Jefferies, E., Van Overwalle, F., Vogeley, K., Mars, R.B., Turetsky, B.I., Laird, A.R., Fox, P.T., Eickhoff, S.B., Bzdok, D., 2018. Computing the social brain connectome across systems and states. Cereb. Cortex 28 (7), 2207–2232. doi:10.1093/cercor/bhx121.

Alkire, D., Levitas, D., Warnell, K.R., Redcay, E., 2018. Social interaction recruits mentalizing and reward systems in middle childhood. Hum. Brain Mapp. 39 (10), 3928–3942.

Arioli, M., Cattaneo, Z., Ricciardi, E., Canessa, N., 2021. Overlapping and specific neural correlates for empathizing, affective mentalizing, and cognitive mentalizing: a coordinate-based meta-analytic study. Hum. Brain Mapp. 42 (14), 4777–4804. doi:10.1002/hbm.25570.

Arslan, S., Ktena, S.I., Makropoulos, A., Robinson, E.C., Rueckert, D., Parisot, S., 2018. Human brain mapping: a systematic comparison of parcellation methods for the human cerebral cortex. Neuroimage 170 (April 2017), 5–30. doi:10.1016/j.neuroimage.2017.04.014.

Assem, M., Glasser, M. F., Van Essen, D. C., & Duncan, J. (2020). A domain-general cognitive core defined in multimodally parcellated human cortex. Cerebral Cortex, 30(8), 4361-4380.

Barrett, L.F., Satpute, A.B., 2013. Large-scale brain networks in affective and social neuroscience: towards an integrative functional architecture of the brain. Curr. Opin. Neurobiol. 23 (3), 361–372. doi:10.1016/j.conb.2012.12.012.

Beckmann, C.F., 2012. Modelling with independent components. Neuroimage 62 (2), 891–901. doi:10.1016/j.neuroimage.2012.02.020.

Beckmann, C.F., Beckmann, C.F., Smith, S.M., Smith, S.M., 2004. Probabilistic independent component analysis for functional magnetic resonance imaging. IEEE Trans. Med. Imaging 23, 137–152. doi:10.1109/TMI.2003.822821.

Bhaganagarapu, K., Jackson, G.D., Abbott, D.F., 2013. An automated method for identifying artifact in independent component analysis of resting-state FMRI. Front. Hum. Neurosci. 7 (July), 343. doi:10.3389/fnhum.2013.00343.

Bhaganagarapu, K., Jackson, G.D., Abbott, D.F., 2014. De-noising with a SOCK can improve the performance of event-related ICA. Front. Neurosci. 8 (September), 1–9. doi:10.3389/fnins.2014.00285.

Binney, R.J., Ramsey, R., 2020a. Social Semantics: the role of conceptual knowledge and cognitive control in a neurobiological model of the social brain. Neurosci. Biobehav. Rev. 112 (March 2019), 28–38. doi:10.1016/j.neubiorev.2020.01.030.

Binney, R.J., Ramsey, R., 2020b. Social Semantics: the role of conceptual knowledge and cognitive control in a neurobiological model of the social brain. Neurosci. Biobehav. Rev. 112 (January), 28–38. doi:10.1016/j.neubiorev.2020.01.030.

Braun, U., Schäfer, A., Walter, H., Erk, S., Romanczuk-Seiferth, N., Haddad, L., Schweiger, J.I., Grimm, O., Heinz, A., Tost, H., Meyer-Lindenberg, A., Bassett, D.S., 2015. Dynamic reconfiguration of frontal brain networks during executive cognition in humans. In: Proceedings of the National Academy of Sciences of the United States of America, 112, pp. 11678–11683. doi:10.1073/pnas.1422487112.

Bressler, S.L., Menon, V., 2010. Large-scale brain networks in cognition: emerging methods and principles. Trends Cogn. Sci. (Regul. Ed.) 14 (6), 277–290. doi:10.1016/j.tics.2010.04.004.

Buckner, R.L., DiNicola, L.M., 2019. The brain's default network: updated anatomy, physiology and evolving insights. Nat. Rev. Neurosci. 20 (10), 593–608. doi:10.1038/s41583-019-0212-7.

Cai, W., Warren, S.L., Duberg, K., Pennington, B., Hinshaw, S.P., Menon, V., 2021. Latent brain state dynamics distinguish behavioral variability, impaired decision-making, and inattention. Mol. Psychiatry 26 (9), 4944–4957. doi:10.1038/s41380-021-01022-3.

Ciaramidaro, A., Becchio, C., Colle, L., Bara, B.G., Walter, H., 2014. Do you mean me? Communicative intentions recruit the mirror and the mentalizing system. Soc. Cogn. Affect Neurosci. 9 (7), 909–916. doi:10.1093/scan/nst062.

Ciric, R., Nomi, J.S., Uddin, L.Q., Satpute, A.B., 2017. Contextual connectivity: a framework for understanding the intrinsic dynamic architecture of large-scale functional brain networks. Sci. Rep. 7 (1), 1–16. doi:10.1038/s41598-017-06866-w.

Cole, M.W., Bassett, D.S., Power, J.D., Braver, T.S., Petersen, S.E., 2014. Intrinsic and task-evoked network architectures of the human brain. Neuron 83 (1), 238–251. doi:10.1016/j.neuron.2014.05.014.

Cole, M.W., Ito, T., Bassett, D.S., Schultz, D.H., 2016. Activity flow over resting-state networks shapes cognitive task activations. Nat. Neurosci. 19 (12), 1718–1726. doi:10.1038/nn.4406.

Cotter, J., Granger, K., Backx, R., Hobbs, M., Looi, C.Y., Barnett, J.H., 2018. Social cognitive dysfunction as a clinical marker: a systematic review of meta-analyses across 30 clinical conditions. Neurosci. Biobehav. Rev. 84 (October 2017), 92–99. doi:10.1016/j.neubiorev.2017.11.014.

Diveica, V., Koldewyn, K., Binney, R.J., 2021. Establishing a role of the semantic control network in social cognitive processing: a meta-analysis of functional neuroimaging studies. Neuroimage 245 (November), 118702. doi:10.1016/j.neuroimage.2021.118702.

Dixon, M.L., De La Vega, A., Mills, C., Andrews-Hanna, J., Spreng, R.N., Cole, M.W., Christoff, K., 2018. Heterogeneity within the frontoparietal control network and its relationship to the default and dorsal attention networks. In: Proceedings of the National Academy of Sciences of the United States of America, 115, pp. E1598–E1607. doi:10.1073/pnas.1715766115.

Du, Y., Pearlson, G.D., Yu, Q., He, H., Lin, D., Sui, J., Wu, L., Calhoun, V.D., 2016. Interaction among subsystems within default mode network diminished in schizophrenia patients: a dynamic connectivity approach. Schizophr. Res. 170 (1), 55–65. doi:10.1016/j.schres.2015.11.021.

Duncan, J., 2010. The multiple-demand (MD) system of the primate brain: mental programs for intelligent behaviour. Trends Cogn. Sci. (Regul. Ed.) 14 (4), 172–179. doi:10.1016/j.tics.2010.01.004.

Ezaki, T., Himeno, Y., Watanabe, T., Masuda, N., 2021. Modelling state-transition dynamics in resting-state brain signals by the hidden Markov and Gaussian mixture models. Eur J Neurosci 54 (4), 5404–5416.

Feng, C., Eickhoff, S.B., Li, T., Wang, L., Becker, B., Camilleri, J.A., Hétu, S., Luo, Y., 2021. Common brain networks underlying human social interactions: evidence from large-scale neuroimaging meta-analysis. Neurosci. Biobehav. Rev. 126 (July 2020), 289–303. doi:10.1016/j.neubiorev.2021.03.025.

Ghahramani, Z., Beai, M.J., 2000. Variational inference for Bayesian mixtures of factor analysers. Adv. Neural Inf. Process Syst. 449–455.

Gonzalez-Castillo, J., Bandettini, P.A., 2018. Task-based dynamic functional connectivity: recent findings and open questions. Neuroimage 180 (August 2017), 526–533. doi:10.1016/j.neuroimage.2017.08.006.

Hardwick, R.M., Caspers, S., Eickhoff, S.B., Swinnen, S.P., 2018. Neural correlates of action: comparing meta-analyses of imagery, observation, and execution. Neurosci. Biobehav. Rev. 94 (August), 31–44. doi:10.1016/j.neubiorev.2018.08.003.

Hari, R., Henriksson, L., Malinen, S., Parkkonen, L., 2015. Centrality of social interaction in human brain function. Neuron 88 (1), 181–193.

Hari, R., Kujala, M.V., 2009. Brain basis of human social interaction: from concepts to brain imaging. Physiol. Rev. 89 (2), 453–479.

Hutchison, R.M., Womelsdorf, T., Allen, E.a., Bandettini, P.a., Calhoun, V.D., Corbetta, M., Della Penna, S., Duyn, J.H., Glover, G.H., Gonzalez-Castillo, J., Handwerker, D.a., Keilholz, S., Kiviniemi, V., Leopold, D.A., de Pasquale, F., Sporns, O., Walter, M., Chang, C., 2013a. Dynamic functional connectivity: promise, issues, and interpretations. Neuroimage 80, 360–378. doi:10.1016/j.neuroimage.2013.05.079.

Hutchison, R.M., Womelsdorf, T., Allen, E.a., Bandettini, P.a., Calhoun, V.D., Corbetta, M., Della Penna, S., Duyn, J.H., Glover, G.H., Gonzalez-Castillo, J., Handwerker, D.a., Keilholz, S., Kiviniemi, V., Leopold, D.a., de Pasquale, F., Sporns, O., Walter, M., Chang, C., 2013b. Dynamic functional connectivity: promise, issues, and interpretations. Neuroimage 80, 360–378. doi:10.1016/j.neuroimage.2013.05.079.

Hyatt, C.J., Calhoun, V.D., Pittman, B., Corbera, S., Bell, M.D., Rabany, L., Pelphrey, K., Pearlson, G.D., Assaf, M., 2020. Default mode network modulation by mentalizing in young adults with autism spectrum disorder or schizophrenia. NeuroImage Clin. 27 (June), 102343. doi:10.1016/j.nicl.2020.102343.

Iraji, A., Faghiri, A., Lewis, N., Fu, Z., Rachakonda, S., Calhoun, V.D., 2021. Tools of the trade: estimating time-varying connectivity patterns from fMRI data. Soc. Cogn. Affect Neurosci. 16 (8), 849–874. doi:10.1093/scan/nsaa114.

Jenkinson, M., Bannister, P., Brady, M., Smith, S., 2002. Improved optimization for the robust and accurate linear registration and motion correction of brain images. Neuroimage 17 (2), 825–841. doi:10.1006/nimg.2002.1132.

Kennedy, D.P., Adolphs, R., 2012. The social brain in psychiatric and neurological disorders. Trends Cogn. Sci. (Regul. Ed.) 16 (11), 559–572. doi:10.1016/j.tics.2012.09.006.

Krendl, A.C., Betzel, R.F., 2022. Social cognitive network neuroscience. Soc. Cogn. Affect Neurosci. 17 (5), 510–529. doi:10.1093/scan/nsac020.

Krishnan, A., Williams, L.J., McIntosh, A.R., Abdi, H., 2011. Partial Least Squares (PLS) methods for neuroimaging: a tutorial and review. Neuroimage 56 (2), 455–475. doi:10.1016/j.neuroimage.2010.07.034.

Kwon, S., Watanabe, M., Fischer, E., Bartels, A., 2017. Attention reorganizes connectivity across networks in a frequency specific manner. Neuroimage 144 (March 2016), 217–226. doi:10.1016/j.neuroimage.2016.10.014.

Lamm, C., Decety, J., Singer, T., 2011. Meta-analytic evidence for common and distinct neural networks associated with directly experienced pain and empathy for pain. Neuroimage 54 (3), 2492–2502. doi:10.1016/j.neuroimage.2010.10.014.

Lee, B., Cai, W., Young, C.B., Yuan, R., Ryman, S., Kim, J., Santini, V., Henderson, V.W., Poston, K.L., Menon, V., 2022. Latent brain state dynamics and cognitive flexibility in older adults. Prog. Neurobiol. 208 (April 2021), 102180. doi:10.1016/j.pneurobio.2021.102180.

Li, W., Mai, X., Liu, C., 2014. The default mode network and social understanding of others: what do brain connectivity studies tell us. Front. Hum. Neurosci. 8 (1 FEB), 1–15. doi:10.3389/fnhum.2014.00074.

Lurie, D.J., Kessler, D., Bassett, D.S., Betzel, R.F., Breakspear, M., Kheilholz, S., Kucyi, A., Liégeois, R., Lindquist, M.A., McIntosh, A.R., Poldrack, R.A., Shine, J.M., Thompson, W.H., Bielczyk, N.Z., Douw, L., Kraft, D., Miller, R.L., Muthuraman, M., Pasquini, L., Calhoun, V.D., 2020. Questions and controversies in the study of time-varying functional connectivity in resting fMRI. Netw. Neurosci. 4 (1), 30–69. doi:10.1162/netn_a_00116.

Lynch, C.J., Power, J.D., Scult, M.A., Dubin, M., Gunning, F.M., Liston, C., 2020. Rapid precision functional mapping of individuals using multi-echo fMRI. Cell Rep. 33 (12), 108540. doi:10.1016/j.celrep.2020.108540.

McIntosh, aR., Bookstein, F.L., Haxby, J.V., Grady, C.L, 1996. Spatial pattern analysis of functional brain images using partial least squares. Neuroimage 3 (3), 143–157. doi:10.1006/nimg.1996.0016, Pt 1.

McIntosh, A.R., Lobaugh, N.J., 2004. Partial least squares analysis of neuroimaging data: applications and advances. Neuroimage 23 (1), S250–S263. doi:10.1016/j.neuroimage.2004.07.020, Suppl.

Mejia, A.F., Nebel, M.B., Wang, Y., Caffo, B.S., Guo, Y., 2020. Template independent component analysis: targeted and reliable estimation of subject-level brain networks using big data population priors. J. Am. Stat. Assoc. 115 (531), 1151–1177. doi:10.1080/01621459.2019.1679638.

Menon, V., D'Esposito, M., 2022. The role of PFC networks in cognitive control and executive function. Neuropsychopharmacology 47 (1), 90–103. doi:10.1038/s41386-021-01152-w.

Mesulam, M. M. (1990). Large-scale neurocognitive networks and distributed processing for attention, language, and memory. Annals of Neurology: Official Journal of the American Neurological Association and the Child Neurology Society, 28(5), 597-613.

Misaki, M., Kerr, K.L., Ratliff, E.L., Cosgrove, K.T., Simmons, W.K., Morris, A.S., Bodurka, J., 2021. Beyond synchrony: the capacity of fMRI hyperscanning for the study of human social interaction. Soc. Cogn. Affect Neurosci. 16 (1–2), 84–92. doi:10.1093/scan/nsaa143.

Molapour, T., Hagan, C.C., Silston, B., Wu, H., Ramstead, M., Friston, K., Mobbs, D., 2021. Seven computations of the social brain. Soc. Cogn. Affect Neurosci. 16 (8), 745–760. doi:10.1093/scan/nsab024.

Molenberghs, P., Johnson, H., Henry, J.D., Mattingley, J.B., 2016. Understanding the minds of others: a neuroimaging meta-analysis. Neurosci. Biobehav. Rev. 65, 276–291. doi:10.1016/j.neubiorev.2016.03.020.

Molnar-szakacs, I., Uddin, L.Q., 2022. Neuroscience and biobehavioral reviews anterior insula as a gatekeeper of executive control. Neurosci. Biobehav. Rev. 139 (March), 104736. doi:10.1016/j.neubiorev.2022.104736.

Power, J.D., Schlaggar, B.L., Petersen, S.E., 2015. Recent progress and outstanding issues in motion correction in resting state fMRI. Neuroimage 105, 536–551. doi:10.1016/j.neuroimage.2014.10.044.

Pruim, R.H.R., Mennes, M., Buitelaar, J.K., Beckmann, C.F., 2015. Evaluation of ICA-AROMA and alternative strategies for motion artifact removal in resting state fMRI. Neuroimage 112, 278–287. doi:10.1016/j.neuroimage.2015.02.063.

Raichle, M.E., 2015. The brain's default mode network. Annu. Rev. Neurosci. 38, 433–447. doi:10.1146/annurev-neuro-071013-014030.

Raichle, M.E., MacLeod, A.M., Snyder, A.Z., Powers, W.J., Gusnard, D.A., Shulman, G.L., 2001. A default mode of brain function. In: Proceedings of the National Academy of Sciences of the United States of America, 98, pp. 676–682. doi:10.1073/pnas.98.2.676.

Ramsey, R., Ward, R., 2020. Putting the nonsocial into social neuroscience: a role for domain-general priority maps during social interactions. Perspect. Psychol. Sci. 15 (4), 1076–1094. doi:10.1177/1745691620904972.

Redcay, E., Dodell-Feder, D., Pearrow, M.J., Mavros, P.L., Kleiner, M., Gabrieli, J.D., Saxe, R., 2010. Live face-to-face interaction during fMRI: a new tool for social cognitive neuroscience. Neuroimage 50 (4), 1639–1647.

Redcay, E., Schilbach, L., 2019. Using second-person neuroscience to elucidate the mechanisms of social interaction. Nat. Rev. Neurosci. 20 (8), 495–505. doi:10.1038/s41583-019-0179-4.

Schaefer, A., Kong, R., Gordon, E.M., Laumann, T.O., Zuo, X.N., Holmes, A.J., Eickhoff, S.B., Yeo, B.T.T., 2018. Local-global parcellation of the human cerebral cortex from intrinsic functional connectivity MRI. Cereb. Cortex 28 (9), 3095–3114. doi:10.1093/cercor/bhx179.

Schilbach, L., Eickhoff, S.B., Rotarska-Jagiela, A., Fink, G.R., Vogeley, K., 2008. Minds at rest? Social cognition as the default mode of cognizing and its putative relationship to the "default system" of the brain. Conscious Cogn. 17 (2), 457–467. doi:10.1016/j.concog.2008.03.013.

Schilbach, L., 2014. On the relationship of online and offline social cognition. Front. Hum. Neurosci. 8 (MAY), 1–8. doi:10.3389/fnhum.2014.00278.

Schilbach, L. (2016). Towards a second-person neuropsychiatry. Philosophical Transactions of the Royal Society B: Biological Sciences, 371(1686), 20150081.

Schilbach, L., Timmermans, B., Reddy, V., Costall, A., Bente, G., Schlicht, T., Vogeley, K., 2013. Toward a second-person neuroscience. Behav. Brain Sci. 36 (4), 393–414. doi:10.1017/S0140525X12000660.

Schurz, M., Aichhorn, M., Martin, A., Perner, J., 2013. Common brain areas engaged in false belief reasoning and visual perspective taking: a meta-analysis of functional brain imaging studies. Front. Hum. Neurosci. 7 (NOV), 1–14. doi:10.3389/fnhum.2013.00712.

Schurz, M., Maliske, L., Kanske, P., 2020. Cross-network interactions in social cognition: a review of findings on task related brain activation and connectivity. Cortex 130, 142–157. doi:10.1016/j.cortex.2020.05.006.

Schuwerk, T., Döhnel, K., Sodian, B., Keck, I.R., Rupprecht, R., Sommer, M., 2014. Functional activity and effective connectivity of the posterior medial prefrontal cortex during processing of incongruent mental states. Hum. Brain Mapp. 35 (7), 2950–2965. doi:10.1002/hbm.22377.

Seeley, W.W., Menon, V., Schatzberg, A.F., Keller, J., Glover, G.H., Kenna, H., Reiss, A.L.,

Greicius, M.D., 2007. Dissociable intrinsic connectivity networks for salience processing and executive control. J. Neurosci. 27 (9), 2349–2356. doi:10.1523/JNEUROSCI.5587-06.2007.

Sha, Z., Wager, T.D., Mechelli, A., He, Y., 2019. Common dysfunction of large-scale neurocognitive networks across psychiatric disorders. Biol. Psychiatry 85 (5), 379–388. doi:10.1016/j.biopsych.2018.11.011.

Shamay-Tsoory, S.G., Mendelsohn, A., 2019. Real-life neuroscience: an ecological approach to brain and behavior research. Perspect. Psychol. Sci. 14 (5), 841–859. doi:10.1177/1745691619856350.

Spadone, S., Della Penna, S., Sestieri, C., Betti, V., Tosoni, A., Perrucci, M.G., Romani, G.L., Corbetta, M., 2015. Dynamic reorganization of human resting-state networks during visuospatial attention. In: Proceedings of the National Academy of Sciences of the United States of America, 112, pp. 8112–8117. doi:10.1073/pnas.1415439112.

Sperduti, M., Guionnet, S., Fossati, P., Nadel, J., 2014. Mirror neuron system and mentalizing system connect during online social interaction. Cogn. Process 15 (3), 307–316. doi:10.1007/s10339-014-0600-x.

Špiláková, B., Shaw, D.J., Czekóová, K., Brázdil, M., 2019. Dissecting social interaction: dual-fMRI reveals patterns of interpersonal brain-behavior relationships that dissociate among dimensions of social exchange. Soc. Cogn. Affect. Neurosci. 14 (2), 225–235. doi:10.1093/scan/nsz004.

Špiláková, B., Shaw, D.J., Czekóová, K., Mareček, R., Brázdil, M., 2020. Getting into sync: data-driven analyses reveal patterns of neural coupling that distinguish among different social exchanges. Hum. Brain. Mapp. 41 (4), 1072–1083. doi:10.1002/hbm.24861.

Spreng, R.N., Stevens, W.D., Chamberlain, J.P., Gilmore, A.W., Schacter, D.L., 2010. Default network activity, coupled with the frontoparietal control network, supports goal-directed cognition. Neuroimage 53 (1), 303–317. doi:10.1016/j.neuroimage.2010.06.016.

Taghia, J., Cai, W., Ryali, S., Kochalka, J., Nicholas, J., Chen, T., Menon, V., 2018. Uncovering hidden brain state dynamics that regulate performance and decision-making during cognition. Nat. Commun. 9 (1), 1–53. doi:10.1038/s41467-018-04723-6.

Taghia, J., Ryali, S., Chen, T., Supekar, K., Cai, W., Menon, V., 2017. Bayesian switching factor analysis for estimating time-varying functional connectivity in fMRI. Neuroimage 155 (March), 271–290. doi:10.1016/j.neuroimage.2017.02.083.

Thomas Yeo, B.T., Krienen, F.M., Sepulcre, J., Sabuncu, M.R., Lashkari, D., Hollinshead, M., Roffman, J.L., Smoller, J.W., Zöllei, L., Polimeni, J.R., Fisch, B., Liu, H., Buckner, R.L, 2011. The organization of the human cerebral cortex estimated by intrinsic functional connectivity. J. Neurophysiol. 106 (3), 1125–1165. doi:10.1152/jn.00338.2011.

Timmers, I., Park, A.L., Fischer, M.D., Kronman, C.A., Heathcote, L.C., Hernandez, J.M., Simons, L.E., 2018. Is empathy for pain unique in its neural correlates? A meta-analysis of neuroimaging studies of empathy. Front. Behav. Neurosci. 12 (November), 1–12. doi:10.3389/fnbeh.2018.00289.

Uddin, L.Q., Yeo, B.T.T., Spreng, R.N., 2019. Towards a universal taxonomy of macro-scale functional human brain networks. Brain Topogr. 32 (6), 926–942. doi:10.1007/s10548-019-00744-6.

Urchs, S., Armoza, J., Moreau, C., Benhajali, Y., St-Aubin, J., Orban, P., Bellec, P., 2019. MIST: a multi-resolution parcellation of functional brain networks. MNI Open Res. 1 (May), 3. doi:10.12688/mniopenres.12767.2.

van Dijk, K.R.A., Sabuncu, M.R., Buckner, R.L., 2012. The influence of head motion on intrinsic functional connectivity MRI. Neuroimage 59 (1), 431–438. doi:10.1016/j.neuroimage.2011.07.044.

Van Overwalle, F., 2009. Social cognition and the brain: a meta-analysis. Hum. Brain Mapp. 30 (3), 829–858. doi:10.1002/hbm.20547.

Vossel, S., Geng, J.J., Fink, G.R., 2014. Dorsal and ventral attention systems: distinct neural circuits but collaborative roles. Neuroscientist 20 (2), 150–159. doi:10.1177/1073858413494269.

Wallot, S., Leonardi, G., 2018. Analyzing multivariate dynamics using cross-recurrence quantification analysis (crqa), diagonal-cross-recurrence profiles (dcrp), and multidimensional recurrence quantification analysis (mdrqa)-a tutorial in r. Front. Psychol. 9, 2232.

Yeshurun, Y., Nguyen, M., Hasson, U., 2021. The default mode network: where the idiosyncratic self meets the shared social world. Nat. Rev. Neurosci. 22 (3), 181–192. doi:10.1038/s41583-020-00420-w.

Zhou, Y., Friston, K.J., Zeidman, P., Chen, J., Li, S., Razi, A., 2018. The hierarchical organization of the default, dorsal attention and salience networks in adolescents and young adults. Cereb. Cortex 28 (2), 726–737. doi:10.1093/cercor/bhx307.